ORIGINAL RESEARCH ARTICLE

Giant Dielectric Response in MWCNT/Chitosan Composite Films

Jin Han[1] · Yongfa Wang[1] · Yanran Ma[1] · Chunchang Wang[1]

Abstract

In this work, xMWCNT/chitosan composite films with multi-walled carbon nanotubes (MWCNT) as filler and chitosan as matrix were prepared via a solution blending method. Varied content of MWCNT of 0, 0.5 wt.%, 1 wt.% and 1.5 wt.% was investigated. The dielectric properties of the films were investigated in the temperature range of −60°C to 60°C and frequency range of 10^2–10^6 Hz. The experimental results show that the incorporation of MWCNT can effectively improve the dielectric properties of the film, with optimal results when the content of MWCNT is close to the percolation threshold. A giant dielectric constant (GDC) was found in all the samples and was studied by dielectric and impedance measurements. Maxwell Wagner relaxation was observed in all samples, which is caused by space charges at different interfaces. The GDC is thought to be related to a Maxwell–Wagner relaxation caused by sample–electrode contact. The addition of MWCNT can enhance the Maxwell–Wagner relaxation. The largest enhancement was found in the sample with 1 wt.% MWCNT.

Keywords MWCNT/chitosan · dielectric properties · composite · Maxwell–Wagner relaxation

Introduction

Dielectric materials with a giant dielectric constant (GDC) have important application prospects in information technology, power engineering, energy storage devices, and other fields. An ideal GDC material not only possesses a high dielectric constant, usually larger than 10^3, but also has low dielectric loss, high breakdown strength, and good processing performance.[1–3]

Chitosan is the product of N-deacetylation of chitin. It contains a large number of –OH and –NH$_2$ groups, and the –OH and –NH$_2$ groups can easily participate in chemical reactions.[4,5] Thus, it can be combined with other functional materials to enhance its performance.[6] Chitosan has good solubility, biocompatibility, and degradability,[7] and it also has a wide range of biological pharmacological activity, such as antioxidant behavior, immune regulation, and antitumor activity.[8–10] As a natural renewable resource, chitosan has a wide range of potential applications.[11]

In recent years, the exploration and research of carbon nanotube/biomolecular matrix composites for biological applications has increased rapidly. By integrating the properties of bioactive molecules (enzymes, proteins, DNA, etc.) and carbon nanotubes, it has gradually become a new research hotspot.[12] The multi-walled carbon nanotube (MWCNT) is famous for its excellent thermal, mechanical, and electrical properties. MWCNT has unique mechanical properties and great surface area per unit volume, and it has been proved to be an ideal filler to enhance the electrical properties of polymers.[13,14] In addition, MWCNT shows high conductivity due to its large surface area.[15,16] By adding only a small amount of conductive MWCNT, the dielectric constant of the composite can be significantly improved while maintaining the mechanical flexibility of the composite.[17] MWCNT is a kind of conductive filler. Generally speaking, the dielectric constant of the polymer composite increases with the increase in the filler content and can reach a large value several orders of magnitude greater than the pristine polymer as the content trends to the percolation threshold. When the amount of the conductive filler is over a specific value, the filler particles will join together to form conductive paths, and the composite is transformed from an insulator to a conductor. In this case, the amount of the filler particles is regarded as the seepage threshold.[18]

✉ Chunchang Wang
  ccwang@ahu.edu.cn

1 Laboratory of Dielectric Functional Materials, School
  of Materials Science and Engineering, Anhui University,
  Hefei 230601, China

In recent years, with the progress and rapid growth of microelectronics technology, GDC materials have become increasingly important in the fields of electronics, motors, and electricity. Dielectric materials are widely studied for modern capacitors and have potential applications in modern microelectronics and high-density energy storage.[19,20] Functional devices made of these dielectric materials have been developed towards miniaturization, light weight, high integration, and stabilization. This gives rise to urgent requirements for the comprehensive properties of dielectric materials, such as high dielectric performance, easy processing, low cost, high energy saving, environmental protection efficiency, and good mechanical performance. Only in this way can the energy storage efficiency and working efficiency of the integrated circuit be rapidly improved.[21]

In this paper, composite films with different MWCNT content are prepared using chitosan as matrix and MWCNT as filler, and the effect of MWCNT content on the dielectric properties of the composites is investigated.

Experimental

Materials

Chitosan was supplied by Rhawn with a deacetylation degree $\geq 95\%$ and viscosity of 10–200 mPa·s. MWCNT was supplied by Shenzhen Suiheng Technology Co., Ltd., with a molecular weight of 12.01.

Sample Preparation and Testing

Two grams of chitosan powder was added to 100 mL 1% acetic acid solution. A magnetic stirrer was used to continuously stir the mixture at 40°C for several hours until the chitosan powder was completely dissolved. The solution was then poured into a Petri dish and dried at 50°C to form a chitosan film.

MWCNT in amounts of 0.01 g, 0.02 g, and 0.03 g were weighed and added to 100 mL 1% acetic acid solutions, stirred and subjected to ultrasonication until they formed evenly dispersed mixed solutions. Next, 2.00 g of chitosan powder was added into the above three groups of mixed solutions. The mixture was stirred continuously with a magnetic stirrer for several hours at 40°C until the chitosan and MWCNT were fully dissolved. The solution was then poured into a Petri dish and dried at 50°C to form three different groups of chitosan-MWCNT hybrid films. The phase purity of the MWCNT/chitosan films was tested by x-ray diffraction (XRD, Rigaku SmartLab, Rigaku Beijing Corporation, Beijing, China). The surface morphology of the MWCNT/chitosan films was observed by field emission scanning electron microscopy (FESEM, Regulus8230, Hitachi High-Tech

Corporation, Tokyo, Japan). The Fourier transform infrared (FTIR) spectra of the MWCNT/chitosan films were recorded in the range of 4000–600 cm^{-1} using attenuated total reflection (ATR)-FTIR, (VERTEX 80 + Hyperion 2000, Bruker, Germany). The dielectric properties were analyzed using a Wayne Kerr 6500B impedance analyzer (Wayne Kerr Electronics, Shenzhen, China) with the Partulab DMS-2000 dielectric measurement system (Partulab Technology Co, Wuhan, China).

Results and Discussion

Material Characterization

Figure 1 shows the XRD patterns of composite films with different MWCNT content. The diffraction peak at 26° is the diffraction of the (002) crystal plane of the MWCNT.[22] The diffraction peaks around 14° and 17° are characteristic peaks of chitosan, corresponding to the (020) and (040) crystal planes, respectively. With the increase in the MWCNT content, the characteristic peak of the MWCNT shifts to a lower angle. This indicates that the unit cell parameter and the crystal plane spacing become larger. The pure chitosan shows a certain degree of crystallinity. As the content of MWCNT increases, the peak width decreases and the crystallinity tends to increase. This means that the addition of MWCNT is helpful for the crystallinity. XRD results show that there is a physical interaction rather than a chemical reaction between chitosan and MWCNT.

It is obvious that the dispersion of filler in the polymer matrix is one of the key factors determining the physical properties of the composite.[23] Figure 2 displays the surface SEM images of the MWCNT/chitosan films. As can be seen from Fig. 2, the surface of the pure chitosan film is uniform and dense, which is related to the good film-forming property of the chitosan itself. When MWCNT is added, fibrous materials are observed, and with the increase in MWCNT content, an increasing number of fibrous materials are visible in the field of vision and a slight agglomeration phenomenon appears.

Figure 3 shows the FTIR spectra of the MWCNT/chitosan films. The wide absorption band of pure chitosan appears near 3168 cm^{-1} due to the joint action of O–H and N–H stretching vibrations. C–H stretching vibrations occur at 2916 cm^{-1} and 2852 cm^{-1}. The peak near 1740 cm^{-1} corresponds to the C=O stretching vibration of the carboxyl group. The peak at 1544 cm^{-1} corresponds to the N–H bending vibration, and the peaks appearing around 1164 cm^{-1} and 1052 cm^{-1} correspond to the stretching vibration of C–O–C in chitosan.[24–26] FTIR results show that the binding between chitosan and MWCNT occurs mainly through physical action rather than chemical reactions.
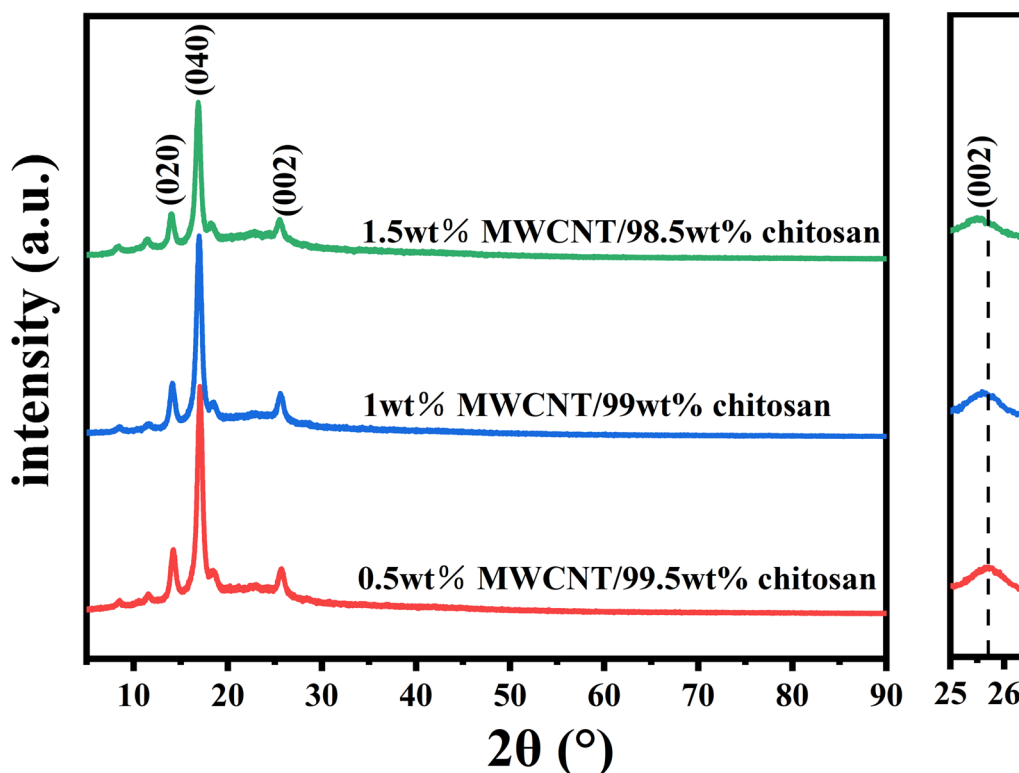
Fig. 1 XRD patterns of the MWCNT/chitosan films.

Dielectric Properties

Figure 4 shows the variations of the dielectric constant (ε', left) and dielectric loss (tan δ, right) with frequency of the MWCNT/chitosan films measured under different temperatures ranging from −60°C to 60°C. It can be seen from Fig. 4 that the dielectric constant of all the samples decreases with increasing frequency. This behavior becomes more significant as the measurement temperature increases. When the measurement temperature rises above ~20°C, a rapid decrease in ε' accompanied by a peak in dielectric loss can be seen in the low-frequency range. This dielectric phenomenon is characterized by a Maxwell–Wagner feature of a steplike change in dielectric constant accompanied by a peak in dielectric loss. The Maxwell–Wagner polarization, also called interfacial polarization, is well known to be caused by space charge locating at interfaces in an inhomogeneous medium due to the differences in the dielectric constant and conductivity.[27] The peak moves to higher frequencies with increasing measurement temperature, indicating that there is a Maxwell–Wagner relaxation in the samples. It is worth noting that the appearance of the Maxwell–Wagner relaxation leads to a rapid increase in the dielectric constant from dozens to more than 1000, giving rise to GDC behavior for all the samples. The GDC behavior depends on the MWCNT content. For example, the dielectric constant at 60°C and 100 Hz for the sample of pure chitosan is 1267.08, which increases to 1352.09 for the sample with 0.5 wt.% MWCNT, achieves a maximum value of 11,647.80 for the sample with 1 wt.% MWCNT, and then decreases to 6478.92 for the sample with 1.5 wt.% MWCNT. This finding demonstrates that the addition of MWCNT can effectively enhance the GDC behavior, and the best GDC behavior is obtained in the sample with 1 wt.% MWCNT.

According to Koop's theory, the dielectric structure of the present samples can be seen as an inhomogeneous medium which consists of two Maxwell–Wagner type layers.[28] Although the MWCNT has good conductivity, it is well separated by the chitosan matrix with poor conductivity. The composite film, therefore, can be regarded as a good insulator when the content of MWCNT is below the percolation threshold. Under an applied alternating electric field, the electrons in the film will be blocked by the sample–electrode interface creating space charge therein. With the increase in the frequency of the alternating electric field, the direction of electron aggregation will change faster, so the space charge polarization decreases, resulting in a decrease in the dielectric constant of the tested material.[29]

Figure 5 shows temperature dependence of the dielectric constant (left) and dielectric loss (right) of the MWCNT/chitosan films in the temperature range of −60°C to 60°C and the frequency range of 10^2–10^6 Hz.
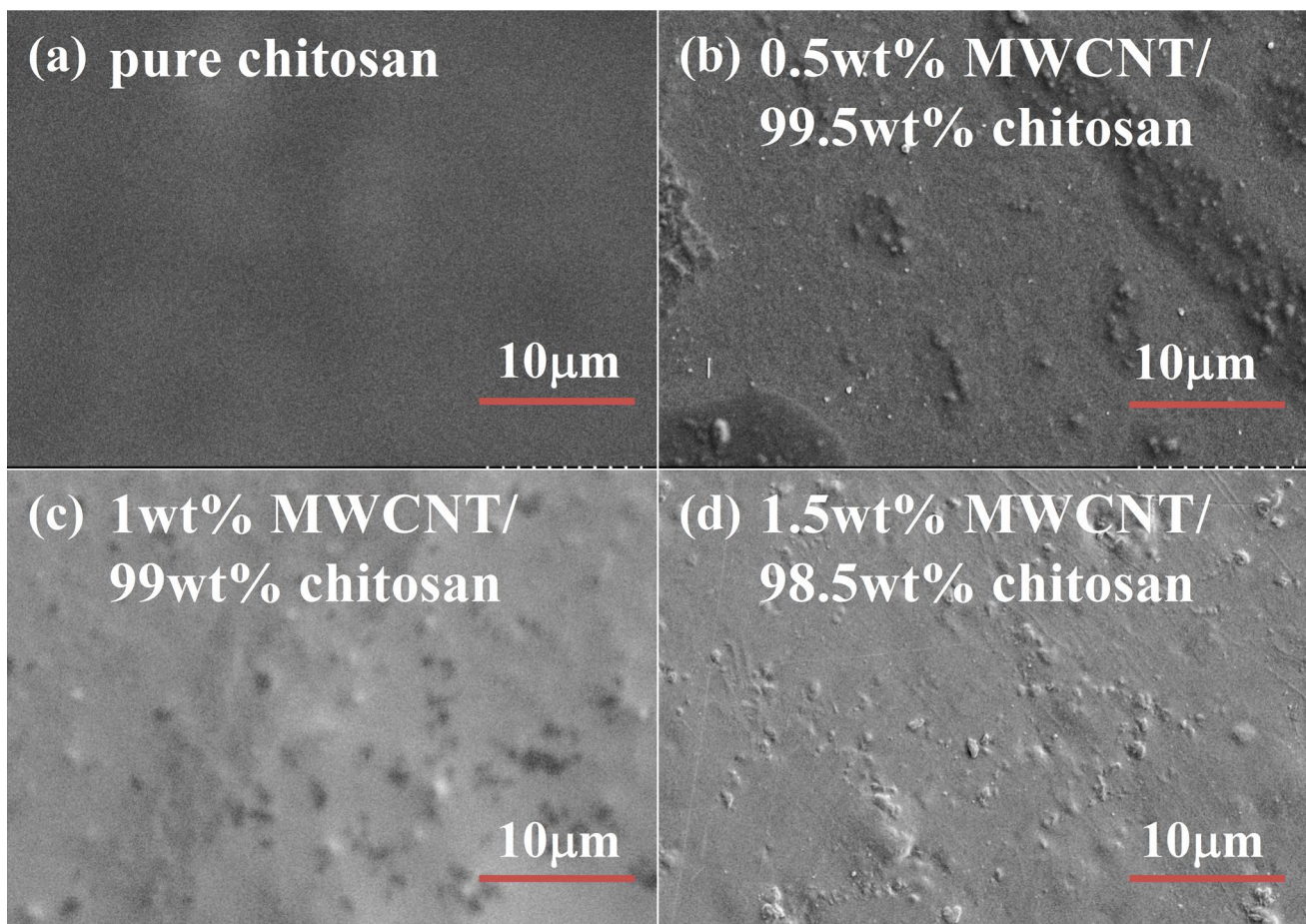
Fig. 2 (a)–(d) SEM surface morphology images of the MWCNT/chitosan films.

All the samples exhibit GDC behavior caused by a kink-like increase in the dielectric constant above room temperature. Meanwhile, a set of thermally activated relaxation can be clearly seen. To obtain more information regarding the relaxation, Arrhenius plots of the relaxation were constructed for all the samples, as displayed in Fig. 6. The Arrhenius law is given by

$$f = f_0 \exp\left(E_a/k_B T_m\right) \tag{1}$$

where f_0 is the pre-exponential, k_B is the Boltzmann constant, E_a represents the activation energy, and T_m is the peak temperature in dielectric loss. It can be seen from Fig. 6 that the relaxations of the four samples agree well with the Arrhenius law. The activation energy was calculated to be 0.89 eV, 0.86 eV, 0.87 eV, and 0.95 eV for the samples of pure chitosan, 0.5 wt.% MWCNT/99.5 wt.% chitosan, 1 wt.% MWCNT/99 wt.% chitosan, and 1.5 wt.% MWCNT/98.5 wt.% chitosan, respectively.

Complex Impedance Spectra

To further study the dielectric properties of the films, the impedance spectra of the samples recorded at room temperature under different DC biases were measured and the results are displayed in Fig. 7. It can be seen that the Nyquist plots (Z″ versus Z′, with Z″ and Z′ being the imaginary and real parts of the complex impedance) of the samples follow a semicircle followed by a low-frequency "tail". This "tail" could be related to the Warburg impedance[30] caused by friction charging effect. The Maxwell–Wagner nature of the thin film can be confirmed through further impedance analysis.[31] The semicircle reflects the relaxation process. The room-temperature Nyquist plots for the samples reveal that the four samples can be clarified into two types: type 1 for samples with low MWCNT content (with MWCNT content = 0 wt.% and 0.5 wt.%) and type 2 for those with high MWCNT
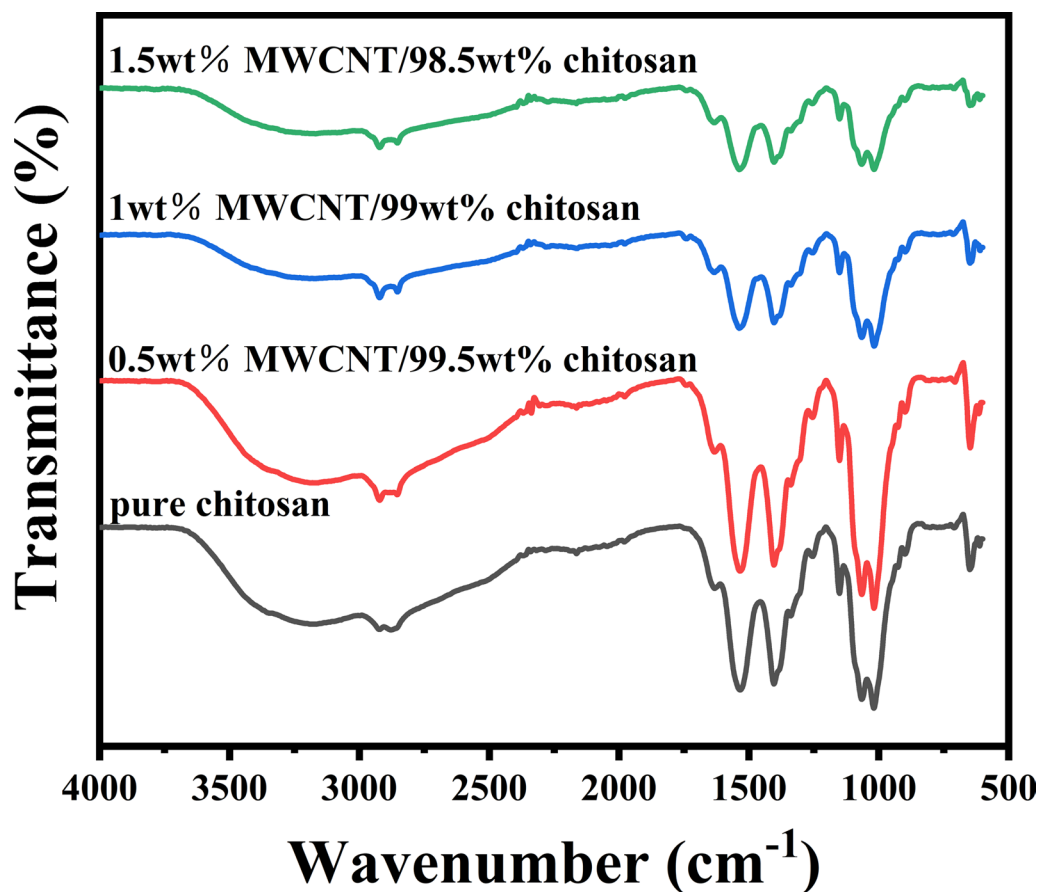
Fig. 3 FTIR spectra of the MWCNT/chitosan films.

content (with MWCNT content = 1.0 wt.% and 1.5 wt.%). For type 1 samples, a small DC bias of 1 V can significantly depress the Nyquist plot. When the DC bias is higher than 1 V, the Nyquist plot is gradually enhanced by the bias. On the other hand, for type 2 samples, a remarkable enhancement in the Nyquist plot is seen for bias less than 1 V, followed by gentle enhancement for the biases higher than 1 V. It is well known that the Maxwell–Wagner relaxation is associated with a Schottky barrier that can be effectively tuned by a DC bias.[30] The above result firmly indicates that the observed relaxation is a Maxwell–Wagner relaxation, which is caused by space charge at the various interfaces. There are two main interfaces in the present samples: MWCNT/chitosan interface and sample–electrode contact. As the relaxation also appears in the pure chitosan sample without the MWCNT/chitosan interface, the former case can be excluded. Therefore, we can safely come to the conclusion that the observed relaxation is a Maxwell–Wagner relaxation caused by sample–electrode contact.

AC Conductivity

To further confirm the above conclusion, an AC conductivity investigation was performed. Figure 8 shows the variations in AC conductivity with frequency of the MWCNT/chitosan films. At the same temperature and frequency, as the MWCNT content increases, the conductivity first increases and then decreases. This is because, as a conductive dopant, the addition of MWCNT can improve the conductive property of the composite. However, when the MWCNT content is too large, the additional charge will be blocked at the sample–electrode contact due to the Maxwell–Wagner relaxation. The electrostatic field yielded by the blocked charges (namely space charge) strongly prevents further charge movement towards the electrode, thereby reducing the conductive property. It can be seen that all the samples exhibit good linear behavior with a slope close to unity in the temperature range below ca. 30°C. This is a typical feature known as nearly constant loss (NCL).[32] Beyond this temperature, an upwardly inclined sigmoidal

Fig. 4 (a)–(d) Frequency dependence of the dielectric constant of the MWCNT/chitosan films recorded at different temperatures. (e)–(h) Frequency dependence of the dielectric loss of the MWCNT/chitosan films recorded at different temperatures.
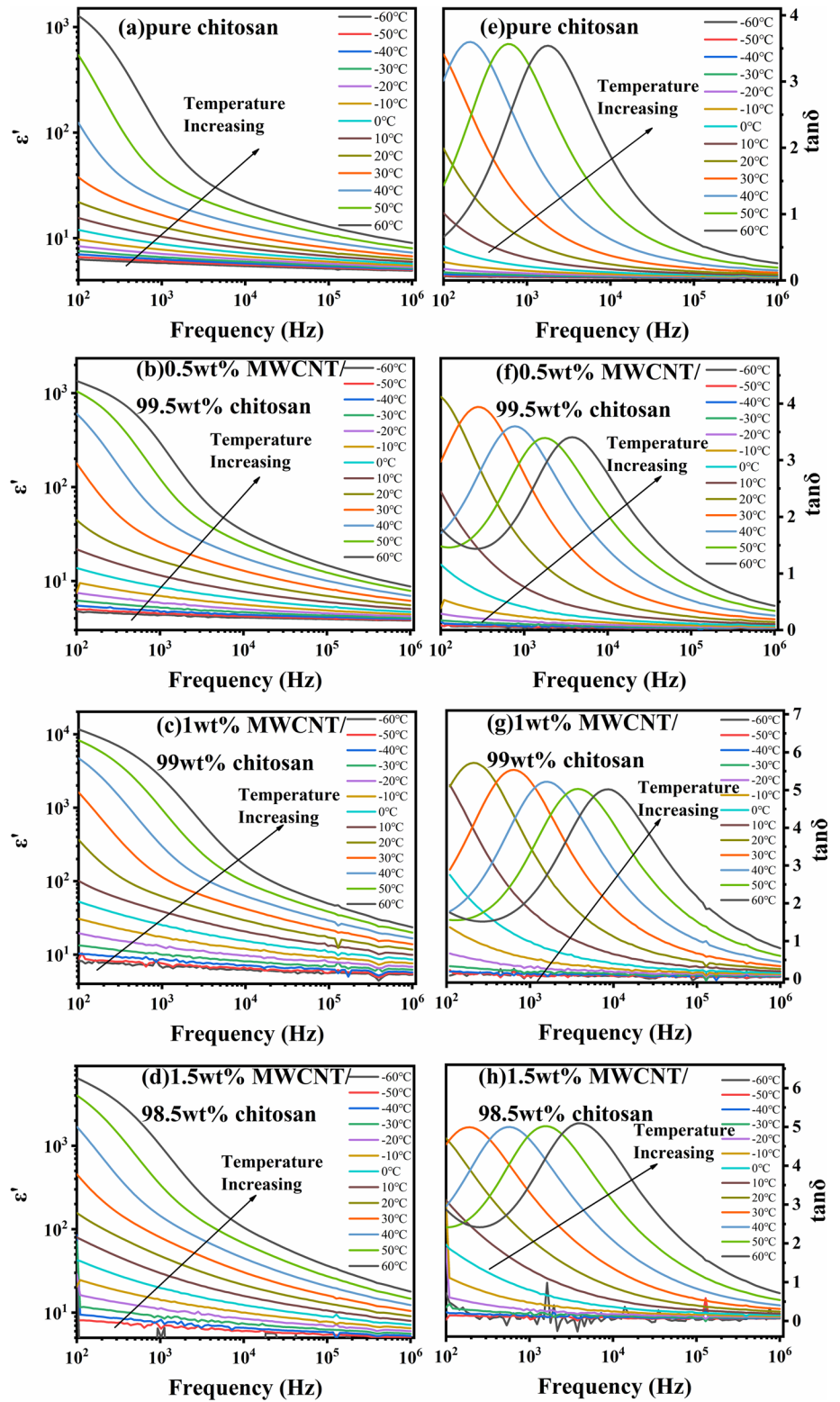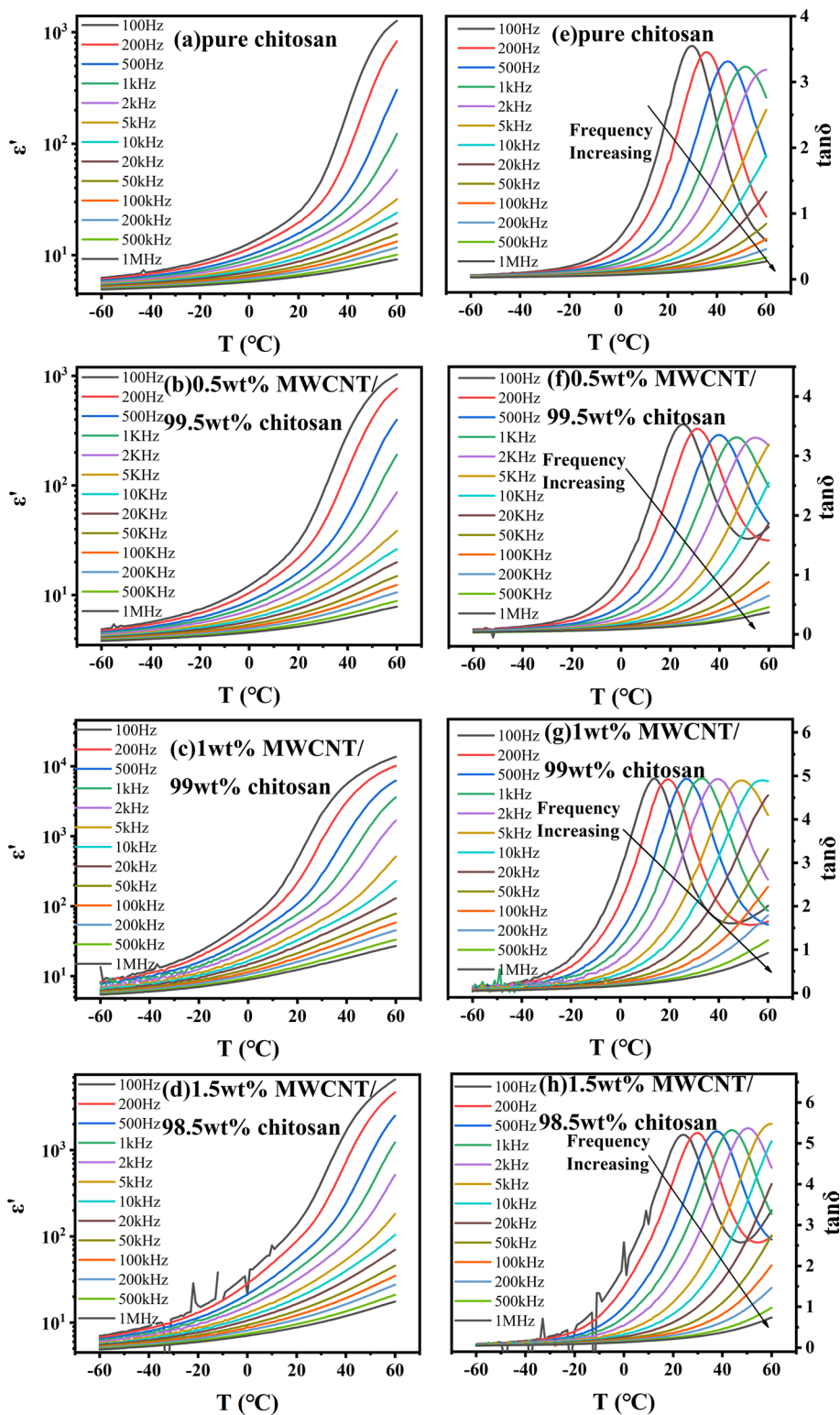
Fig. 5 (a)–(d) Temperature dependence of the dielectric constant of the MWCNT/chitosan films. (e)–(h) Temperature dependence of the dielectric loss of the MWCNT/chitosan films.
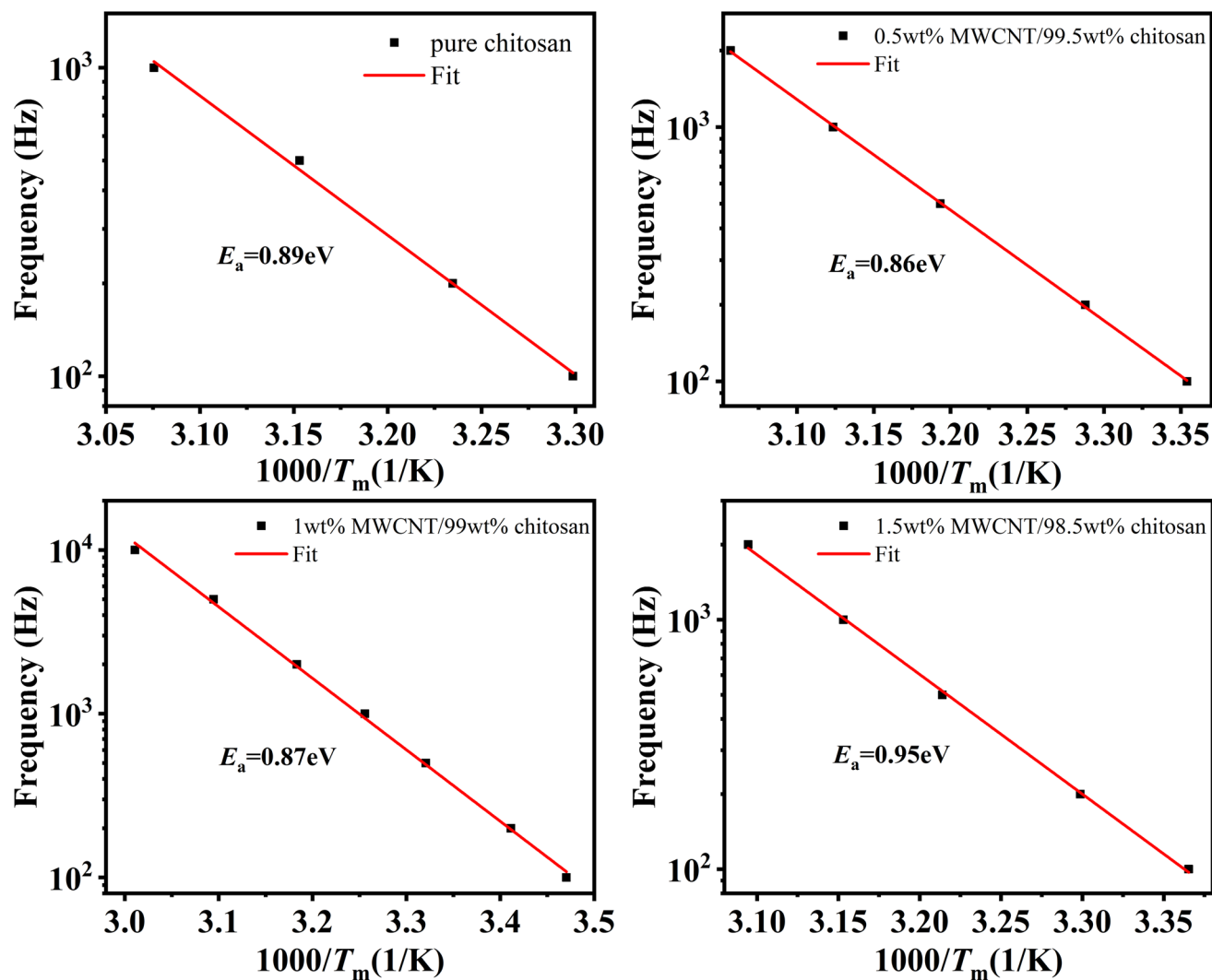
Fig. 6 The Arrhenius plots of the MWCNT/chitosan films.

curve appears and is superimposed on the linear line. The sigmoidal curve for AC conductivity is the hallmark for Maxwell–Wagner relaxation,[33] which leads to a steplike increase in AC conductivity at low frequencies. For example, when the temperature rises from 30°C to 60°C, step increases in AC conductivity at 100 Hz of 3.69×10^{-6}, 3.33×10^{-6}, 2.84×10^{-5}, and 1.13×10^{-5} were found for the samples of pure chitosan, 0.5 wt.% MWCNT/99.5 wt.% chitosan, 1 wt.% MWCNT/99 wt.% chitosan, and 1.5 wt.%

MWCNT/98.5 wt.% chitosan, respectively. The largest enhancement was found in the sample with 1 wt.% MWCNT. Since the Maxwell–Wagner relaxation is determined by the difference in conductivity between the sample and electrode, overdoping of the MWCNT will improve the conductivity of the sample, which in turn decreases the conductivity difference and is thereby unfavorable for the Maxwell–Wagner relaxation. This result strongly confirms that the GDC behavior occurs due to the Maxwell–Wagner relaxation.
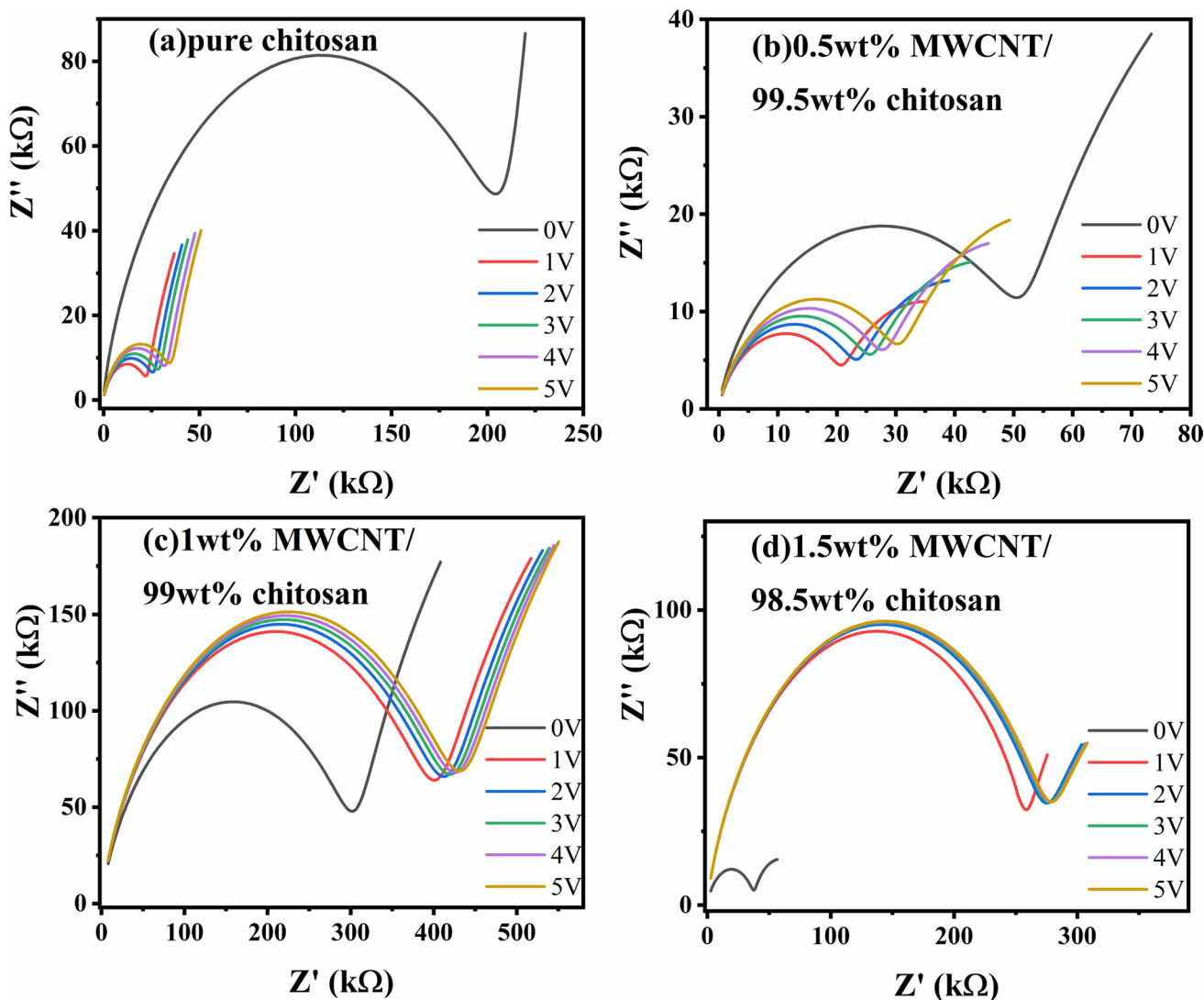
Fig. 7 (a)–(d) Nyquist plots of the MWCNT/chitosan films recorded at room temperature under different DC bias voltages.

Conclusion

In conclusion, xMWCNT/chitosan composite films with $x = 0$ wt.%, 0.05 wt.%, 0.1 wt.%, and 0.1 5 wt.% were prepared via a solution blending method. Dielectric investigations of the films reveal that all the samples exhibit NCL dielectric behavior in the temperature range below ~30°C and GDC behavior with dielectric constants higher than 10^3 in the temperature range over 30°C. The GDC behavior was firstly enhanced and then weakened by increasing the MWCNT content. The largest dielectric constant of 11,647.80 was achieved at 60°C and 100 Hz in the sample with 1 wt.% MWCNT. The GDC behavior is related to Maxwell–Wagner relaxation caused by sample–electrode contact.
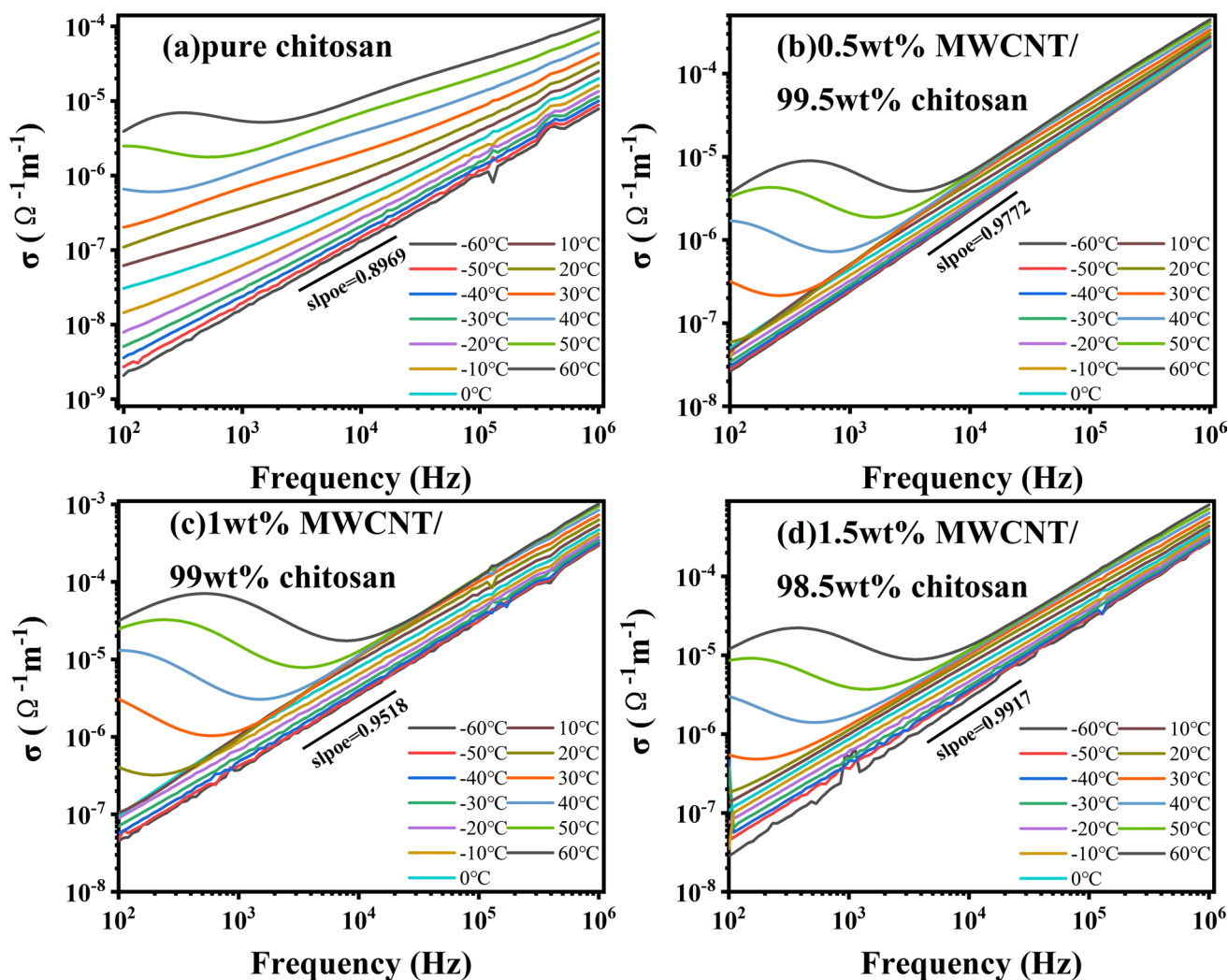
Fig. 8 (a)–(d) The frequency dependence of AC conductivity of the MWCNT/chitosan films recorded at different temperatures.

Author Contributions All authors contributed to the study. Material preparation was performed by YW and YM. Data collection and analysis were performed by JH. The first draft of the manuscript was written by JH. The supervision of the whole work and revision of the manuscript were made by CW.

Date Availability The data that support the findings of this study are available from the corresponding authors upon reasonable request.

Conflict of interest On behalf of all authors, the corresponding author states that there is no conflict of interest.

Ethical Approval Human tissue experiment is not involved in this paper

References

1. X.Y. Huang and P.K. Jiang, Core-shell structured high-k polymer nanocomposites for energy storage and dielectric applications. *Adv. Mater.* 27(3), 546 (2015).

2. B.P. Mandal, P. Anithakumari, S. Nigam, C. Majumder, M. Mohapatra, and A.K. Tyagi, Enhancement of dielectric constant in a niobium doped titania system: an experimental and theoretical study. *New J. Chem.* 40(11), 9526 (2016).

3. P. Mandal and A. Sundaresan, Dielectric relaxation mechanism in high-pressure synthesized $BiCr_{0.5}Mn_{0.5}O_3$. *J. Electron. Mater.* 50, 1615 (2021).

4. F.A. Razmi, N. Ngadi, S. Wong, I.M. Inuwa, and L.A. Opotu, Kinetics, thermodynamics, isotherm and regeneration analysis of chitosan modified pandan adsorbent. *J. Clean. Prod.* 231, 98 (2019).

5. L. Ren, J. Xu, Y. Zhang, J. Zhou, D. Chen, and Z. Chang, Preparation and characterization of porous chitosan microspheres and

adsorption performance for hexavalent chromium. *Int. J. Biol. Macromol.* 135, 898 (2019).

6. T. Fahmy, H. Elhendawi, W.B. Elsharkawy, and F.M. Reicha, AC conductivity and dielectric relaxation of chitosan/poly (vinyl alcohol) biopolymer polyblend. *Bull. Mater. Sci.* 43, 1 (2020).

7. C.K. Pillai, W. Paul, and C.P. Sharma, Chitin and chitosan polymers: Chemistry, solubility and fiber formation. *Prog. Polym. Sci.* 34(7), 641 (2009).

8. G.N. Shi, C.N. Zhang, R. Xu, J.F. Niu, H.J. Song, X.Y. Zhang, W.W. Wang, Y.M. Wang, C. Li, X.Q. Wei, and D.L. Kong, Enhanced antitumor immunity by targeting dendritic cells with tumor cell lysate-loaded chitosan nanoparticles vaccine. *Biomaterials* 113, 191 (2017).

9. R.M.C. Udayangani, S.H.S. Dananjaya, C. Nikapitiya, G.J. Heo, J. Lee, and M. De Zoysa, Metagenomics analysis of gut microbiota and immune modulation in zebrafish (Danio rerio) fed chitosan silver nanocomposites. *Fish Shellfish Immunol.* 66, 173 (2017).

10. L. Wei, W. Tan, G. Wang, Q. Li, F. Dong, and Z. Guo, The antioxidant and antifungal activity of chitosan derivatives bearing Schiff bases and quaternary ammonium salts. *Carbohydr. Polym.* 226, 115256 (2019).

11. C. Choi, S. Kim, P. Pak, D. Yoo, and Y. Chung, Effect of N-acylation on structure and properties of chitosan fibers. *Carbohydr. Polym.* 68(1), 122 (2007).

12. A.M. Esawi and M.M. Farag, Carbon nanotube reinforced composites: potential and current challenges. *Mater. Des.* 28(9), 2394 (2007).

13. L. Yang, J. Qiu, H. Ji, K. Zhu, and J. Wang, Enhanced dielectric and ferroelectric properties induced by TiO_2@MWCNTs nanoparticles in flexible poly (vinylidene fluoride) composites. *Compos. Part A Appl. Sci. Manuf.* 65, 125 (2014).

14. Z.K. Ren, L.W. Liu, M.Y. Zhang, Y.J. Liu, and J.S. Leng, Dielectric and breakdown properties of MWCNT and OMMT-reinforced epoxy composites. *J. Electron. Mater.* 48, 7270 (2019).

15. W. Lu, X. Qin, A.M. Asiri, A.O. Al-Youbi, and X. Sun, Ni foam: a novel three-dimensional porous sensing platform for sensitive and selective nonenzymatic glucose detection. *Analyst* 138(2), 417 (2013).

16. J. Zhu, J. Jiang, J. Liu, R. Ding, Y. Li, H. Ding, Y. Feng, G. Wei, and X. Huang, CNT-network modified Ni nanostructured arrays for high performance non-enzymatic glucose sensors. *RSC Adv.* 1(6), 1020 (2011).

17. C.W. Tang, B. Li, L. Sun, B. Lively, and W.H. Zhong, The effects of nanofillers, stretching and recrystallization on microstructure, phase transformation and dielectric properties in PVDF nanocomposites. *Eur. Polym. J.* 48(6), 1062 (2012).

18. C. Pecharromán, F. Esteban-Betegón, J.F. Bartolomé, S. López-Esteban, and J.S. Moya, New percolative BaTiO3-Ni composites with a high and frequency-independent dielectric constant (εr ≈ 80000). *Adv. Mater.* 13, 1541 (2001).

19. Z.Q. Liu and Z.P. Yang, High permittivity, low dielectric loss and impedance characteristics of $Li_{0.5}La_{0.5}Cu_3Ti_4O_{12}$ ceramics by a sol–gel technique. *J. Electron. Mater.* 48, 5333 (2019).

20. Z.G. He, Simultaneously high dielectric constant and breakdown strength in $CaCu_3Ti_4O_{12}$-filled polymer composites. *J. Electron. Mater.* 51, 4521 (2022).

21. K.R. Mahmoud, H.A. El-Hakim, and A. Abdelaziz, Design of compact double-layer microwave absorber for X-Ku bands using genetic algorithm. *Prog. Electromagn. Res. B* 65, 157 (2016).

22. W. Wu, B. Han, H. Gao, Z. Liu, T. Jiang, and J. Huang, Desulfurization of flue gas: SO_2 absorption by an ionic liquid. *Angew. Chem. Int. Ed.* 43(18), 2415 (2004).

23. R. Mukherjee, R. Sharma, P. Saini, and S. De, Nanostructured polyaniline incorporated ultrafiltration membrane for desalination of brackish water. *Environ. Sci. Water Res. Technol.* 1(6), 893 (2015).

24. L. Vodolazov, V. Shatalov, T. Molchanova, and V. Peganov, Polymerization of uranyl ions and its role in ion-exchange extraction of uranium. *At. Energy* 90(1), 213 (2001).

25. J. Huang, A. Riisager, R.W. Berg, and R. Fehrmann, Tuning ionic liquids for high gas solubility and reversible gas sorption. *J. Mol. Catal. A Chem.* 279(2), 170 (2008).

26. S. Li, Y. Gong, Y. Yang, C. He, L. Hu, L. Zhu, L. Sun, and D. Shu, Recyclable $CNTs/Fe_3O_4$ magnetic nanocomposites as adsorbents to remove bisphenol a from water and their regeneration. *Chem. Eng. J.* 260, 231 (2015).

27. C.C. Wang, M.N. Zhang, and W. Xia, High-temperature dielectric relaxation in Pb(Mg1/3Nb2/3)O3-PbTiO3 single crystals. *J. Am. Ceram. Soc.* 96, 1521 (2013).

28. C.G. Koops, On the dispersion of resistivity and dielectric constant of some semiconductors at audiofrequencies. *Phys. Rev.* 83(1), 121 (1951).

29. R. Tang, C. Jiang, W. Qian, J. Jian, X. Zhang, H. Wang, and H. Yang, Dielectric relaxation, resonance and scaling behaviors in $Sr_3Co_2Fe_{24}O_{41}$ hexaferrite. *Sci. Rep.* 5, 13645 (2015).

30. C.C. Wang, M. He, F. Yang, J. Wen, G.Z. Liu, and H.B. Lu, Enhanced tunability due to interfacial polarization in $La_{0.7}Sr_{0.3}MnO_3/BaTiO_3$ multilayers. *Appl. Phys. Lett.* 90, 192904 (2007).

31. C.C. Wang, W. Ni, D. Zhang, X.H. Sun, J. Wang, H.B. Li, and N. Zhang, Dielectric properties of pure and Mn-doped $CaCu_3Ti_4O_{12}$ ceramics over a wide temperature range. *J. Electroceram.* 36, 46 (2016).

32. M.R. Díaz-Guillén, J.A. Díaz-Guillén, A.F. Fuentes, J. Santamaría, and C. León, Crossover to nearly constant loss in ac conductivity of highly disordered pyrochlore-type ionic conductors. *Phys. Rev. B* 82, 174304 (2010).

33. M. Zhu, N. Zhang, H. Wang, Y.D. Li, S.G. Huang, Q.J. Li, Y. Yu, Y.M. Guo, X.L. Liu, and C.C. Wang, Point-defect-induced colossal dielectric behavior in GaAs single crystals. *RSC Adv.* 7(42), 26130 (2017).